HHS Public Access

Author manuscript

J Photochem Photobiol B. Author manuscript; available in PMC 2017 September 01.

Published in final edited form as:

J Photochem Photobiol B. 2016 September ; 162: 674–680. doi:10.1016/j.jphotobiol.2016.07.028.

A new dual-collimation batch reactor for determination of ultraviolet inactivation rate constants for microorganisms in aqueous suspensions

Stephen B. Martin Jr.[a,b,*], **Elizabeth S. Schauer**[a], **David H. Blum**[c], **Paul A. Kremer**[b], **William P. Bahnfleth**[b], and **James D. Freihaut**[b]

[a]Centers for Disease Control and Prevention, National Institute for Occupational Safety and Health, Respiratory Health Division, Field Studies Branch, 1095 Willowdale Road, Morgantown, WV 26505, USA

[b]Pennsylvania State University, College of Engineering, Department of Architectural Engineering, Indoor Environment Center, 104 Engineering Unit A, University Park, PA 16802, USA

[c]Massachusetts Institute of Technology, Department of Architecture, Building Technology Laboratory, 77 Massachusetts Avenue, Room 5-418, Cambridge, MA 02139, USA

Abstract

We developed, characterized, and tested a new dual-collimation aqueous UV reactor to improve the accuracy and consistency of aqueous k-value determinations. This new system is unique because it collimates UV energy from a single lamp in two opposite directions. The design provides two distinct advantages over traditional single-collimation systems: 1) real-time UV dose (fluence) determination; and 2) simple actinometric determination of a reactor factor that relates measured irradiance levels to actual irradiance levels experienced by the microbial suspension. This reactor factor replaces three of the four typical correction factors required for single-collimation reactors. Using this dual-collimation reactor, *Bacillus subtilis* spores demonstrated inactivation following the classic multi-hit model with k = 0.1471 cm^2/mJ (with 95% confidence bounds of 0.1426 to 0.1516).

Keywords

Ultraviolet; Inactivation rate constant; Collimated-beam reactor; Germicidal; k-Value; *Bacillus subtilis*

[*]Corresponding author at: Centers for Disease Control and Prevention, National Institute for Occupational Safety and Health, Respiratory Health Division, Field Studies Branch, 1095 Willowdale Road, Morgantown, WV 26505, USA. SMartin1@cdc.gov (S.B. Martin).

Disclaimer

The findings and conclusions in this article are those of the authors and do not necessarily represent the views of the National Institute for Occupational Safety and Health (NIOSH). Mention of a specific product or company does not constitute endorsement by NIOSH.

1. Introduction

Although this research focuses on ultraviolet germicidal irradiation (UVGI) systems designed to inactivate microorganisms in air, the roots of UVGI are steeped in the disinfection of water. The first documented use of UV energy to disinfect drinking water occurred in 1909 at Marseilles, France [1]. Seven years later, in 1916, the first UV system in the United States was installed to disinfect 1.136×10^7 L of water per day (3,000,000 gal/day) for the 17,000 residents of Henderson, Kentucky [2]. UV devices used for water treatment have been researched extensively, resulting in solid biodosimetry testing strategies, useful system design criteria, and regulatory oversight. The same cannot be said for UVGI air and surface disinfection systems.

UVGI air-disinfection systems are currently used in schools, offices, healthcare settings, correctional facilities, social-assistance shelters, and homes to improve indoor air quality, reduce airborne disease transmission, and disinfect surfaces. While many successful systems have been installed in various settings, air-disinfection system design is often as much art as science. Accurate ultraviolet (UV) inactivation rate constants (k-values) for microorganisms of interest are essential to proper system design. Inactivation rate constants are species-dependent and relate the susceptibility of a given microorganism population to UV radiation [3–6]. Ideally, k-values used for system design would be determined on the organism(s) of interest suspended in air. However, these results are very difficult to generate, so k-values determined using aqueous organism suspensions are generally used instead.

A collimated-beam UV reactor is often used to determine k-values for microorganisms in aqueous suspensions. While the term “collimated-beam” implies a beam of radiation with truly parallel rays, bench-top systems used for UV experiments do not meet that stringent criterion [7]. Regardless, the term is commonly used to describe UV exposure systems in the scientific literature. Measured k-values for many species of viruses, bacteria, and fungi have been published in the scientific literature [8]. However, no standard methods exist for the determination of k-values, which makes reported values difficult to interpret and apply with certainty to system design. To help UVGI system designers make better decisions, improved standardized methods for k-value determination need to be developed. This work describes a new dual-collimation UV batch reactor design that can improve the accuracy of aqueous k-values over those determined using some classic single-collimation systems.

UV exposure systems used for aqueous microbial inactivation studies typically collimate UV energy in only one direction, which may affect the accuracy of the results in two ways. First, such systems do not allow UV irradiance measurements to be made while the microorganisms are being exposed. Instead, irradiance measurements are taken before and after microorganism exposure. The average of the pre- and post-irradiance levels is assumed to be the irradiance applied to the microorganisms during an actual exposure test. The impact this has on the accuracy of resulting k-value estimates depends on individual reactor design and operation. Second, single-collimation systems require the determination and use of numerous correction factors (CFs) to relate the irradiance readings from a radiometer to the actual irradiance levels experienced by the microbial suspension. Four CFs are generally required for systems equipped with low-pressure mercury UV lamps [7,9]:

1. Reflection Factor–the fraction of incident UV energy that enters the microbial suspension vs. the UV energy reported by the radiometer,
2. Petri Factor–the variation of irradiance over the surface area of the aqueous microbial suspension,
3. Divergence Factor–the divergence of the UV energy from a truly collimated beam, and
4. Water Factor–the UV energy absorbed as the beam passes through the microbial suspension itself.

Including the four CFs in the UV dose calculation, while making the results more accurate, does not account for all aspects of system design or for lamp output variations that might occur during microbial exposures, when the radiometer sensor is not in place to record them. For instance, conducting tests before the lamp output stabilized, lamp output variations caused by control systems or dimmers, or performance issues with the lamp itself, can have an impact on measurement accuracy. To address the above two limitations of single-collimation reactors, and ultimately to improve the accuracy of microbial k-value determinations, we developed, characterized, and conducted microbial testing with a new dual-collimation UV batch reactor.

2. Materials/methods

2.1. Dual-collimation reactor design & construction

The reactor design was conceived as an improvement to an earlier collimated-beam batch reactor fabricated at the Pennsylvania State University Department of Architectural Engineering using key references outlining reactor design and characterization [7,9–12]. The new dual-collimation aqueous phase reactor, shown in Fig. 1 and schematically in Fig. 2, collimates UV energy in two directions, 180° apart. The reactor is built inside an enclosure with interior dimensions of 79.4 cm length × 27.3 cm width × 57.5 cm height; however, the collimated-beam portion within the enclosure has a height of 27.9 cm and is located between two aluminum shelves that are each 0.6 cm thick. The bottom of the upper shelf and the top of the lower shelf have attached 1.0 cm × 1.0 cm × 0.2 cm wall thickness 6061 anodized aluminum U-channels. These channels hold the collimating plates in place at four desired locations on either side of the lamp. The interior of the reactor enclosure is painted flat black to minimize unwanted UV reflections.

The reactor contains two sockets for testing with either a Philips (Roosendaal, Netherlands) 18 W (TUV PL-L 18W/4P) or 35 W (TUV PL-L 35 W/4P HO) low-pressure mercury lamp positioned in the center of the reactor, and oriented perpendicular to the collimated-beam assembly. While only one lamp is used at a time, the lamp sockets are positioned in the reactor such that the 18 W lamp extends upward from the lower shelf and the 35 W lamp extends downward from the top shelf. This makes switching between the lamps quick and easy.

To create a pseudo-collimated beam of UV-C radiation directed at both the sample cuvette and the radiometer detector, 27.3 cm wide × 27.3 cm tall × 0.6 cm thick unpainted,

furniture-grade plywood collimating plates with 3.8 cm high × 3.8 cm wide apertures were used. The collimating plates are held in place by sliding them into the aluminum U-channels attached to the upper and lower shelves of the enclosure. There are 22 channels and 4 wooden slats on either side of the lamp. The extra channels allow for variation in the wooden slat positions, if desired.

To precisely control the passage of UV radiation through both collimating paths, a combination of foam padding and shutters were used. Custom-fitted neoprene foam lining the reactor enclosure doors prevented light leakage around the wooden slats. Upon locking of the reactor enclosure doors, the foam is pressed against the wooden slats, creating the light seal. Vincent Associates (Rochester, NY, USA) model CS65S3T1 electronic shutters integrated into the first collimating plate on each side of the lamp precisely control the UV radiation through each of the two collimating paths. These 65 mm aperture iris shutters operate electromechanically to open in 29 ms and are driven by a Vincent Associates Uniblitz VMM-D3 Three Channel Shutter Driver, which was interfaced to the overall reactor control system.

The new dual-collimated-beam UV reactor was designed to expose microbial suspensions inside quartz cuvettes (Part # CQS114, VitroCom, Mountain Lakes, NJ). These cuvettes measured 1.4 cm square (internal) × 6.0 cm high with a wall thickness of 0.13 cm. Small 0.25 cm × 1.2 cm magnetic stir bars were placed inside the cuvettes before covering them with a small loose-fitting, non-reflective cap. To expose the microbial suspension, one cuvette at a time was placed into a housing station equipped with a magnetic stirrer that positioned the cuvette in the center of the collimating apertures for UV exposure testing, while ensuring the microbial suspension was well mixed. The cuvette housing station was constructed of 0.2 cm thick aluminum sections attached by stainless steel machine screws. A 1.9 cm × 1.9 cm square hole was cut into the top portion of the housing station to hold the cuvette in place. A 12 V DC motor with a shaft mounted dual-disc magnet holder was attached to the housing station underneath the cuvette. This served as a magnetic stirrer to spin the small Teflon-coated magnetic stir bar placed inside the cuvette to mix the microorganism suspension during testing. Two parallel 0.3 cm wide slots 17.1 cm apart were milled into the bottom shelf of the reactor. Two machine screws with wing nuts mount the cuvette housing station to the bottom shelf while allowing horizontal adjustment capabilities. Slots in the cuvette and motor housing sections of the holder allowed for independent adjustment of these sections with respect to each other as needed. The 12 V DC stirring motor is attached to a pulse-width modulating, DC speed controller that allows fine-tuned speed control of the magnetic stirring.

The front edge of the cuvette sample and the calibration plane of the ILT1700 (International Light Technologies, Peabody, MA) research radiometer detector head are each located 27.9 cm from the lamp center and they are centered in the collimating apertures. To align and maintain the calibration plane of the radiometer detector head an equal distance from the lamp as the front face of the quartz cuvettes, the detector was mounted onto a custom sensor mounting station. The station was comprised of an anodized aluminum polytetrafluoroethylene-lined guide block and rail system that allowed for vertical adjustment. The detector was attached to a 7.6 cm × 6.4 cm × 0.5 cm thick aluminum plate

by two 1.6 cm long 6–32 zinc-plated steel flat machine screws. The aluminum plate was attached to the guide block by four 2.5 cm long 8–32 stainless steel flat machine screws. The rail was mounted to a 6063 aluminum square angle with 5.1 cm leg lengths and 0.5 cm wall thickness. Two parallel 0.3 cm wide slots, 5.1 cm apart were milled into the bottom shelf of the reactor collimating section. These slots allowed the aluminum angle to be mounted to the bottom shelf with wing nuts and machine screws to provide horizontal adjustment capabilities.

A Vaisala (Helsinki, Finland) model HMT 100, 0% to 100% and −40 °C to 80 °C relative humidity (RH) and temperature sensor probe was used to measure the RH (although virtually irrelevant for aqueous samples) and temperature inside the reactor enclosure during microbial exposure tests. The 1.3 cm diameter sensor probe was mounted in the back right corner of the reactor enclosure behind the cuvette housing station, where it was protected from exposure to UV radiation.

Reactor monitoring and control is achieved through a custom-written National Instruments (Austin, TX) LabVIEW 10 interface. Using the LabVIEW control panel, the user can operate each shutter, operate the lamp, select the communications port for and read irradiance measurements from the radiometer, edit the UV dose desired for each test and the associated reactor correction factors for the irradiance measurements, and exit the program. While in operation, the LabVIEW interface provides real-time monitoring of the UV dose delivered to the microbial sample in the quartz cuvette, and can terminate a test once a preselected UV dose has been achieved. Additionally, the interface has the capability of recording data to a tab-delimited text file that can be opened in most spreadsheet programs.

2.2. Reactor characterization

Once the new aqueous-phase, dual-collimated-beam UV reactor was constructed, it needed to be characterized before it was used for microbial testing. The dual-collimated-beam design of the new reactor provides an advantage over traditional single collimation reactors in that it allows the radiometer sensor head to remain in place during actual microbial sample exposure. Since the cuvette sample is exposed while the radiometer is acquiring real-time measurements, it also allows the use of iodide-iodate chemical actinometry to determine one overall correction factor, termed the “Reactor Factor” (RF), that replaces the reflection factor, Petri factor, and divergence factor required for traditional collimated-beam systems.

The iodide-iodate actinometry solution was prepared by mixing 9.96 g of potassium iodide (KI; Catalog #P410-500, Fisher Scientific, Fair Lawn, NJ), 2.14 g of potassium iodate (KIO_3; Catalog #P253-100, Fisher Scientific, Fair Lawn, NJ), and 0.381 g of borax ($Na_2B_4O_7{\cdot}10H_2O$; Catalog #S248-500, Fisher Scientific, Fair Lawn, NJ) in 100 mL of distilled, deionized water for several minutes until the solids were dissolved [13]. To conduct an individual test, 3 mL of the unexposed solution were pipetted into a standard 1 cm path length disposable methacrylate cuvette (Fisherbrand model 14-955-126, Fisher Scientific, Fair Lawn, NJ).

The cuvette was then placed inside a Thermo Scientific Genesys 10uv spectrophotometer (Thermo Fisher Scientific, Waltham, MA) and an absorbance reading obtained at a wavelength of 300 nm (A_{300}). From this reading, the molar (M) concentration of iodide (C_{KI}) in the solution could be determined as:

$$\mathrm{C_{KI}(M)} = \frac{A_{300}\ \mathrm{cm^{-1}}}{1.061\mathrm{M^{-1}\ cm^{-1}}} \quad (1)$$

where 1.061 M^{-1} cm^{-1} is the extinction coefficient of KI in 0.1 M iodate at 300 nm [14]. A second absorbance reading at 352 nm ($A_{352,pre}$) was also recorded for later use.

Next, 5 mL of the unexposed actinometry solution were pipetted into a quartz cuvette with a small magnetic stir bar as described above. The cuvette was then placed in the cuvette housing station for testing. All testing was done with the 18 W lamp.

Within the reactor control program, all reactor correction factors were set to values of 1.0, so UV dose was calculated using uncorrected irradiance measurements determined by the ILT1700 radiometer. Then, the lamp was turned on and the left shutter controlling UV radiation to the radiometer sensor was opened. Once the radiometer reported that the lamp output was stable, the right shutter was opened to begin the UV exposure to the actinometry solution in the cuvette. The UV exposure was stopped once the desired uncorrected UV dose was reached. After each UV exposure, 3 mL of the exposed solution from the quartz cuvette were pipetted into a new disposable methacrylate cuvette and the absorbance at 352 nm was determined again ($A_{352,post}$) using the Genesys 10uv spectrophotometer. The change in absorbance at 352 nm ($A_{352\Delta}$) was determined as:

$$A_{352\Delta} = A_{352,\mathrm{post}} - A_{352,\mathrm{pre}} \quad (2)$$

Using the calculated value for $A_{352\Delta}$, the number of moles of triiodide formed during the UV exposure could be calculated as:

$$[\mathrm{triiodide(mol)}] = \frac{(A_{352\Delta})(\mathrm{V_{sol}})}{\varepsilon} \quad (3)$$

where V_{sol} is the volume of actinometry solution exposed in liters (0.005 L in this case) and ε is the molar absorption coefficient or molar extinction coefficient with units of M^{-1} cm^{-1}. For the results presented here, ε = 26,400 M^{-1} cm^{-1} was used, as originally reported by Rahn [14] and used in much of the related published literature. Rahn later published a revised value of ε = 27,600 M^{-1} cm^{-1} [15], which, upon recalculation of the results, reduced the estimated UV dose experienced by the chemical actinometer (and subsequently by the *Bacillus subtilis* spores described below) by 3.8%.

The quantum yield (Φ) of the actinometer represents the number of moles of triiodide formed per mole of photons absorbed. Previous work has shown that Φ depends on the

iodide concentration in the solution (C_{KI}) as well as the temperature of the solution (T_{sol}, assumed the same as the temperature measured by the Vaisala HMT 100 probe mounted inside the reactor) as follows [14]:

$$\Phi(\text{mol/einstein}) = 0.75[1 + 0.02(T_{sol} - 20.7)] \times [1 + 0.23(C_{KI} - 0.577)] \quad (4)$$

Finally, the UV dose received by the actinometry solution inside the quartz cuvette (D_{ACT}) is calculated to be:

$$D_{ACT} = \frac{(4.72 \times 10^8)\,(A_{352\Delta})(V_{sol})}{\varepsilon \Phi (A_{sol})} \quad (5)$$

where 4.72×10^8 is the number of millijoules per einstein (mJ/einstein) of 254 nm photons, and A_{sol} is the cross-sectional area of actinometry solution exposed to the UV radiation (3.57 cm^2 in this case).

Using the actinometry procedure described above, an RF for the new aqueous-phase system was determined for the new dual-collimation reactor. Five complete sets of actinometry tests were conducted at 13 uncorrected dose levels: 2, 4, 6, 8, 10, 15, 20, 25, 30, 35, 40, 45, and 50 mJ/cm^2. The 13 dose levels were randomized for each set of tests. Linear regression was used to relate the UV dose determined by chemical actinometry to the UV dose calculated from uncorrected radiometer readings.

2.3. Microbiological testing

The new aqueous-phase, dual-collimated-beam reactor, presented above, was used to determine the most appropriate UV inactivation model for *Bacillus subtilis* spores (ATCC 6633) in distilled, deionized water. A fresh, 1.2×10^{10} spores/mL suspension of *Bacillus subtilis* was procured from Presque Isle Cultures (Erie, PA). The UV dose range of interest was from 0 to 50 mJ/cm^2 based on previous research results [16]. Samples were dosed at the same 13 dose points used for the actinometry testing: 2, 4, 6, 8, 10, 15, 20, 25, 30, 35, 40, 45, and 50 mJ/cm^2. The 2 mJ/cm^2 increments between 0 and 10 mJ/cm^2 were selected to help provide definition of any shoulder effects, if applicable. Four replicate sets of tests were conducted. During each of the 13 tests within a replicate (corresponding to the 13 UV dose levels), the UV dose levels were randomized in the order each test was performed.

To prepare the test suspension, the bottle containing the 1.2×10^{10} spores/mL stock suspension was first vortexed for 60 s to ensure that the spores were well mixed and that any large spore clumps were broken apart. Then, 166 μL of the stock were added to 1.83 mL of distilled, deionized water in a 15 mL polystyrene, conical centrifuge tube. This tube, which contained a spore concentration of approximately 1.0×10^9 spores/mL, was vortexed for 15s. Three successive 10-fold serial dilutions (the first two in 15 mL centrifuge tubes and the last in a 50 mL centrifuge tube) then were performed to yield 30 mL of a 1.0×10^6 spores/mL daily test suspension.

From the test suspension, 3 mL were transferred into a 1 cm path-length disposable methacrylate cuvette (Fisherbrand Model 14-955-126, Fisher Scientific, Pittsburgh, PA). A second cuvette was filled with distilled, deionized water for use as a control. The cuvettes were then placed inside a Thermo Scientific Genesys 10uv spectrophotometer (Thermo Fisher Scientific, Waltham, MA) and an absorbance reading (a) for each was obtained at a wavelength of 254 nm. Using these absorbance readings, the water factor (WF) for each suspension was calculated as:

$$\mathrm{WF}=\frac{1-10^{-\mathrm{al}}}{\mathrm{al}\ln(10)} \quad (6)$$

where l = 1.3 cm (the path length through the VitroCom quartz cuvettes used for testing). The WF would account for any UV absorbance resulting from turbidity or color in the microbiological suspension.

To determine the viability of the *Bacillus subtilis* spores during testing, the appropriate samples were plated on Tryptic Soy Agar (TSA) plates. The TSA plates were prepared from BD (Catalog #236950, Becton, Dickenson and Company, Sparks, MD) Tryptic Soy Agar (Soy-bean-Casein Digest Agar) dehydrated media, in accordance with label instructions. Approximately 20 mL of agar were pipetted into each sterile 100 mm disposable, polystyrene Petri dish. Agar plates were stored in the refrigerator for up to one week prior to use.

Just prior to each UV exposure test, samples of the daily test suspension were taken and three serial 10-fold dilutions were performed. The final serial dilution (1:1000) was then plated and cultured in triplicate on TSA plates using a Spiral Biotech (Bethesda, MD) Autoplate Model 3000 spiral plating system. The Autoplate 3000 was operated in the 20 μL Lawn Mode. In this mode, the system deposits 20 μL of the suspension at a constant rate in a tight spiral pattern across the full surface of the agar plate. Use of Lawn Mode results in uniform spore growth over the entire surface of the plate.

Five milliliters of the appropriate test suspension were then transferred into a VitroCom quartz cuvette with the small stir bar added. The cuvette was placed inside the new reactor and the appropriate RF and WF values entered into the control program, which then calculated actual UV dose (D_{UV}) experienced by the test suspension as:

$$D_{UV}=F\times RF\times WF \quad (7)$$

where F is the uncorrected fluence measured by the radiometer.

The 18 W lamp was then turned on and allowed to stabilize. Once the real-time radiometer measurements were determined to be stable, the right shutter was opened and the cuvette containing the suspension was then exposed to UV energy until the control program, integrating real-time corrected radiometer measurements, terminated the exposure at the desired UV dose. Immediately after the UV exposure, samples of the exposed suspension

were taken and appropriate serial 10-fold dilutions were made. The necessary serial dilutions were then plated and cultured in triplicate on TSA plates using the spiral plating system described above. Immediately after plating, all culture plates were placed inside an incubator at 30 °C.

After 18–24 h of incubation, the plates were enumerated. Plate counts for *Bacillus subtilis* spores were considered acceptable when 30 to 300 colonies were present. The average number of colony forming units (CFU) from the three unexposed replicates provided a measure of the number of viable organisms in the suspension prior to UV exposure (N_0). Similarly, samples of the suspension after exposure provided a measure of the number of organisms surviving the UV treatment (N). The survival fraction (S) from each exposure test was then calculated as the ratio of the CFU post-exposure to the CFU prior to exposure (N/N_0).

Once the microbiological data were obtained, model coefficients were obtained using the nonlinear least-squares fitting procedure within the Curve Fitting Toolbox of the MATLAB (version R2013a, MathWorks, Inc., Natick, MA) computing environment. The experimental results were fitted to five separate inactivation models commonly reported in UV inactivation studies, as shown in Table 1. The model with the smallest sum of squares error (SSE) was selected as the most predictive model, as it had the smallest error component.

3. Results

3.1. Reactor characterization

The RF was determined by the straightforward comparison of the UV doses determined by chemical actinometry in the quartz cuvettes and determined from the radiometer readings. This RF incorporates the reflection factor, Petri factor and divergence factor required for typical collimated-beam reactors, along with any small differences attributable to the two opposite collimation paths, into one distinct number. A separate water factor correction is still required. Using Eq. (6) for this study, the values of *a* were 0.008 or less for all test spore suspensions, compared to the distilled, deionized water control. Thus, the water factor was determined to be 0.99. This value for the water factor was used for all *Bacillus subtilis* testing with the new reactor.

The results for the five actinometry trials at each of the 13 doses are shown in Fig. 3. The best-fit regression line is shown, along with the equation of the line and the coefficient of determination (R^2 value). The equation of the line was intentionally forced through the origin (0,0) because the actinometer and radiometer would both indicate a dose of zero when the lamp was off. Fig. 3 shows that the testing results are repeatable. The slope of the resulting line of 1.06 demonstrates that the samples inside the quartz cuvettes were actually being exposed to UV irradiance levels 1.06 times higher than the radiometer sensor was measuring. Thus, multiplying the radiometer sensor measurements by an RF of 1.06 brought the radiometer measurements into agreement with the actual irradiance experienced by samples inside the quartz cuvettes.

Fig. 4 shows the results from a single set of actinometry tests conducted with the RF set to 1.06 in the LabVIEW control program. The resulting slope of 1 (actually 0.9982) confirms that the radiometer was reading virtually the same irradiance level and UV dose as the cuvette samples experienced. Since the lamp was allowed to stabilize prior to exposing the actinometer solution to UV energy, temporal fluctuations in lamp output during a test, if any, were negligible. So, the horizontal error bars represent the ±7.5% accuracy reported for the radiometer on the detector calibration certificates. The vertical error bars represent the ±3.1% uncertainty of the iodide-iodate actinometer reported by the U.S. National Institute of Standards and Technology (NIST) [15].

3.2. Microbiological testing

The results from the four test replicates of aqueous *Bacillus subtilis* survival at each of the 13 UV dose levels are shown in Fig. 5. Roughly 2-logs of inactivation (99%) were achieved at UV doses around 45 mJ/cm^2. There was also a pronounced shoulder effect at UV doses lower than 10 mJ/cm^2.

The experimental results were fitted to the five inactivation models described in Table 1. The multi-hit exponential decay with a shoulder model with n forced to be an integer (model 2) provided the lowest sum of squares error (SSE = 0.1028) and was selected as the most predictive model tested, with k = 0.1471 cm^2/mJ (95% confidence bounds of 0.1426 to 0.1516) and a discrete number of hits required to inactivate the spores (n) of 7. This model fit the data well as indicated by R^2 = 0.9887 and the root mean square error (RMSE) of 0.0449. The computed value for the inactivation rate constant falls within the range of k-values reported by other researchers for *Bacillus subtilis* spores in water when normalized to the exponential decay model with a shoulder (see Table 2).

4. Discussion

This new dual-collimation aqueous batch reactor design provides two distinct advantages over traditional single collimation systems. First, it allows for a real-time UV dose determination. Measuring the dose in real time will capture any UV lamp output variations during exposure tests that might otherwise go unnoticed. It could also reduce the time required between individual tests as researchers would not necessarily need to wait until the lamp is completely stabilized before beginning a test. Knowing the dose in real-time also allows for microbial exposure tests to be terminated at desired dose levels instead of requiring the estimation of the actual dose after a test is completed using the average of before and after test irradiance measurements. The ability to terminate the test at accurate dose levels will allow for more targeted testing of organisms with complex inactivation curves. For instance, shoulders or inflection points in the microbial inactivation curves could be defined more accurately since tests can be terminated at more accurate dose levels around the phenomenon of interest. Secondly, this new dual-collimation design allows for a simple actinometric determination of an overall correction factor, the RF, which relates irradiance levels measured by the radiometer sensor to the irradiance levels experienced by the microbial suspension. The RF replaces three of the four correction factors typically used in single collimation systems, with the water factor being the exception.

These advantages over traditional single-collimation systems could help to improve the accuracy of overall k-value determinations for aqueous microorganisms. The *Bacillus subtilis* results determined using this new reactor fit nicely into the range established by other researchers. By eliminating issues that may affect results determined using some traditional collimated reactors, this new reactor design represents one possible step toward more accurate and repeatable k-value information. However, additional steps are still needed to make reported k-values more reliable for system design. For instance, standardized microbiological procedures, including agar type(s), incubation temperature(s) and time(s), plating method(s), among others, need to be established for microorganisms so results from one study can be directly compared to results from another. Until that time, k-values reported in the literature will remain useful for the study in which they were determined and may not be easily translated to work conducted at other conditions.

References

1. Clemence W. UV at Marseille. Engineering. 1911; 91(106–108):139–142.
2. Smith AT. Ultra-violet rays finish treatment of Henderson water-supply. Eng. News-Rec. 1917; 79:1021–1022.
3. Sharp DG. The lethal action of short ultraviolet rays on several common pathogenic bacteria. J. Bacteriol. 1939; 37:447–460. [PubMed: 16560218]
4. Sharp DG. The effects of ultraviolet light on bacteria suspended in air. J. Bacteriol. 1940; 39:535–547. [PubMed: 16560312]
5. Hollaender A. Effect of long ultraviolet and short visible radiation (3500 to 4900 Å) on *Escherichia coli*. J. Bacteriol. 1943; 46:531–541. [PubMed: 16560737]
6. Jensen MM. Inactivation of airborne viruses by ultraviolet irradiation. Appl. Microbiol. 1964; 12:418–420. [PubMed: 14215971]
7. Bolton JR, Linden KG. Standardization of methods for fluence (UV dose) determination in bench-scale UV experiments. J. Environ. Eng. 2003; 129:209–215.
8. Kowalski, W. Ultraviolet Germicidal Irradiation Handbook. New York: Springer; 2009.
9. Kuo J, Chen C, Nellor M. Standardized collimated beam testing protocol for water/wastewater ultraviolet disinfection. J. Environ. Eng. 2003; 129:774–779.
10. Blatchley ER III. Numerical modelling of UV intensity: application to collimated-beam reactors and continuous-flow systems. Water Res. 1997; 31:2205–2218.
11. Bolton JR, Linden KG. Discussion of “Standardized collimated beam testing protocol for water/wastewater ultraviolet disinfection” by Jeff Kuo, Ching-lin Chen, and Margaret Nellor. J, Environ. Eng. 2005; 131:827.
12. Kuo J, Chen C, Nellor M. Closure to “Standardized collimated beam testing protocol for water/wastewater ultraviolet disinfection” by Jeff Kuo, Ching-lin Chen, and Margaret Nellor. J. Environ. Eng. 2005; 131:828–829.
13. Rahn RO, Bolton J, Stefan MI. The iodide/iodate actinometer in UV disinfection: determination of the fluence rate distribution in UV reactors. Photochem. Photobiol. 2006; 82:611–615. [PubMed: 16613521]
14. Rahn RO. Potassium iodide as a chemical actinometer for 254 nm radiation: use of iodate as an electron scavenger. Photochem. Photobiol. 1997; 66:450–455.
15. Rahn RO, Stefan MI, Bolton JR, Goren E, Shaw P-S, Lykke KR. Quantum yield of the iodide-iodate chemical actinometer: dependence on wavelength and concentration. Photochem. Photobiol. 2003; 78:146–152. [PubMed: 12945582]
16. Nedeljkovic-Davidovic, A. Master of Science Thesis. University Park, PA: Pennsylvania State University; 2008. Fluence Response Curves for *Bacillus subtilis* Spores Applied to UVC Lamps Testing.

17. Kowalski, WJ. Aerobiological Engineering Handbook: A Guide to Airborne Disease Control Technologies. New York, NY: McGraw-Hill; 2006. Ultraviolet germicidal irradiation; p. 231-266.
18. Riley RL, Knight M, Middlebrook G. Ultraviolet susceptibility of BCG and virulent tubercule bacilli. Am. Rev. Respir. Dis. 1976; 113:413–418. [PubMed: 817628]
19. Casarett, AP. Radiation Biology. Englewood Cliffs, NJ: Prentice-Hall, Inc.; 1968.
20. Munakata N, Saito M, Hieda K. Inactivation action spectra of *Bacillus subtilis* spores in extended ultraviolet wavelengths (50–300 nm) obtained with synchrotron radiation. Photochem. Photobiol. 1991; 54:761–768. [PubMed: 1798752]
21. Severin BF, Suidan MT, Engelbrecht RS. Kinetic modeling of U.V. disinfection of water. Water Res. 1983; 17:1669–1678.
22. Fujikawa H, Itoh T. Tailing of thermal inactivation curve of *Aspergillus niger* spores. Appl. Environ. Microbiol. 1996; 62:3745–3749. [PubMed: 8837430]
23. Kowalski, WJ. Aerobiological Engineering Handbook: A Guide to Airborne Disease Control Technologies. New York, NY: McGraw-Hill; 2006. Microbial disinfection fundamentals; p. 143-164.
24. Qualls RG, Johnson JD. Bioassay and dose measurement in UV disinfection. Appl. Environ. Microbiol. 1983; 45:872–877. [PubMed: 6405690]
25. Mamane-Gravetz H, Linden KG, Cabaj A, Sommer R. Spectral sensitivity of *Bacillus subtilis* spores and *MS2 coliphage* for validation testing of ultraviolet reactors for water disinfection. Environ. Sci. Technol. 2005; 39:7845–7852. [PubMed: 16295846]
26. Bohrerova Z, Mamane H, Ducoste JJ, Linden KG. Comparative inactivation of *Bacillus subtilis* spores and MS-2 coliphage in a UV reactor: implications for validation. J. Environ. Eng. 2006; 132:1554–1561.
27. Deguchi K, Yamaguchi S, Ishida H. UV-disinfection reactor validation by computational fluid dynamics and relation to biodosimetry and actinometry. J. Water Environ. Technol. 2005; 3:77–84.

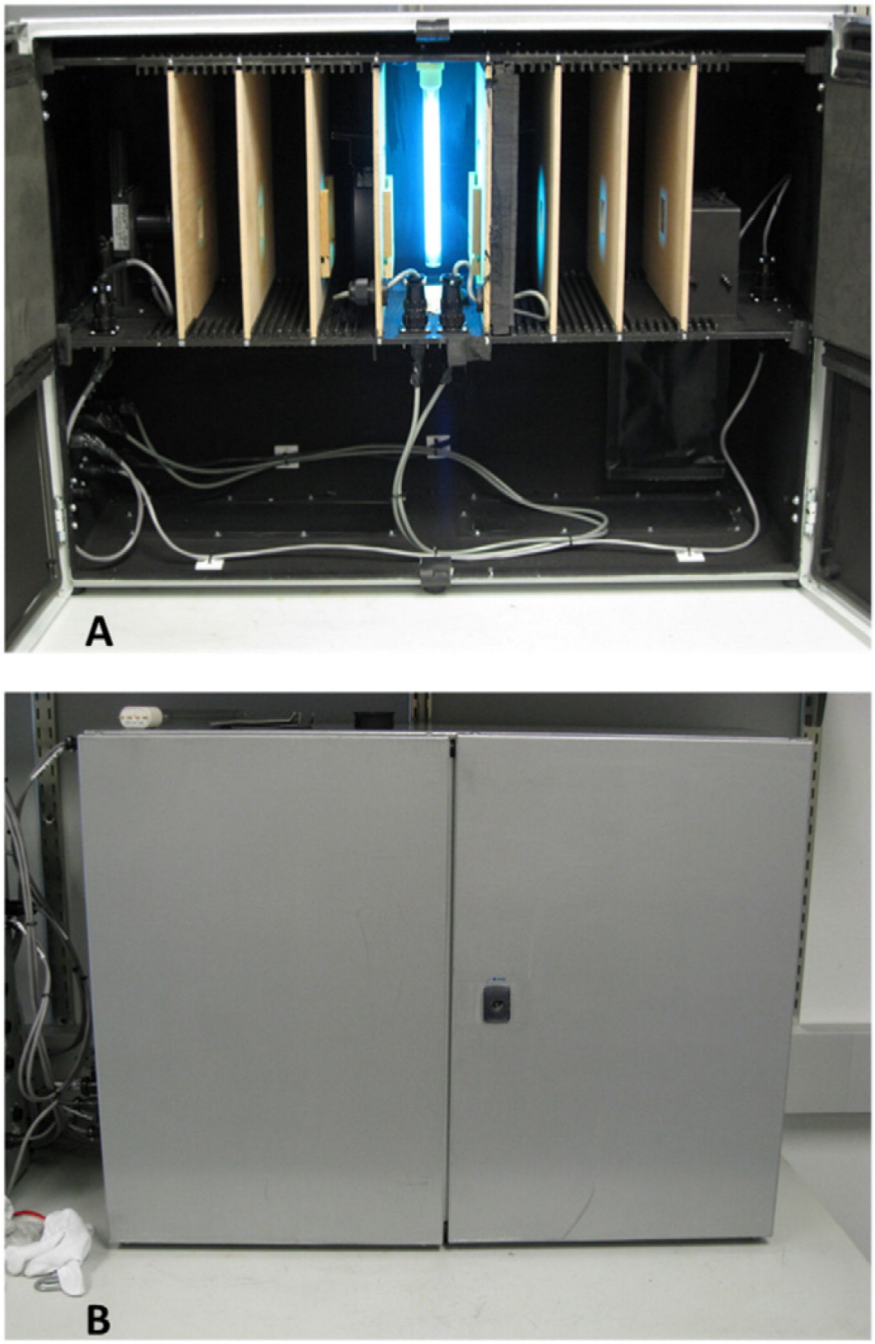

Fig. 1.

Photographs of the new aqueous-phase, dual-collimated-beam UV reactor: A) Reactor with the doors open showing the lamp, dual collimating paths with collimating apertures, sample cuvette housing, and radiometer detector head; B) reactor with the door closed.

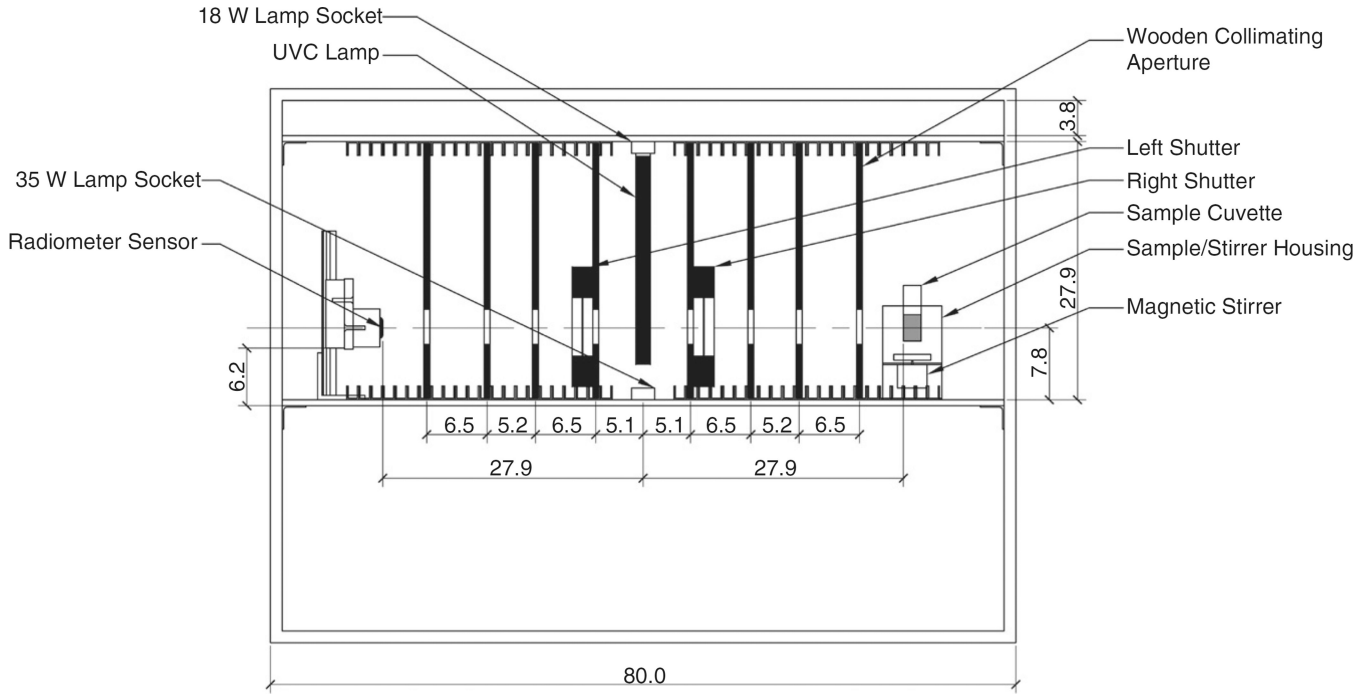

Fig. 2.
Schematic diagram of new dual-collimation UV batch reactor with key dimensions (in cm).

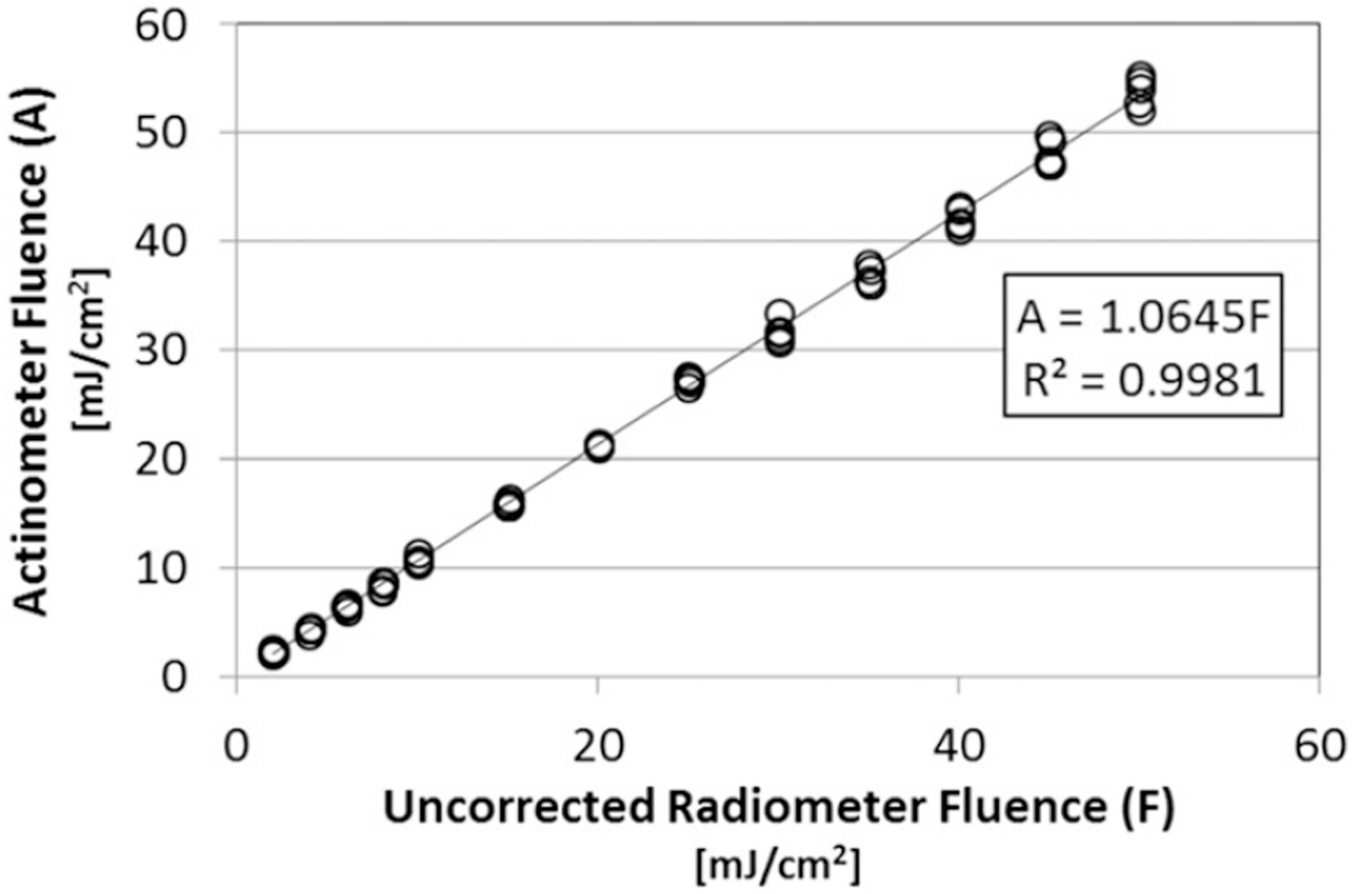

Fig. 3.

Actinometry fluence (A, UV dose) vs. UV dose determined using uncorrected radiometer readings (F); five replicates at each of 13 dose levels. The slope of 1.06 represents the reactor factor necessary to make the two UV dose values equal.

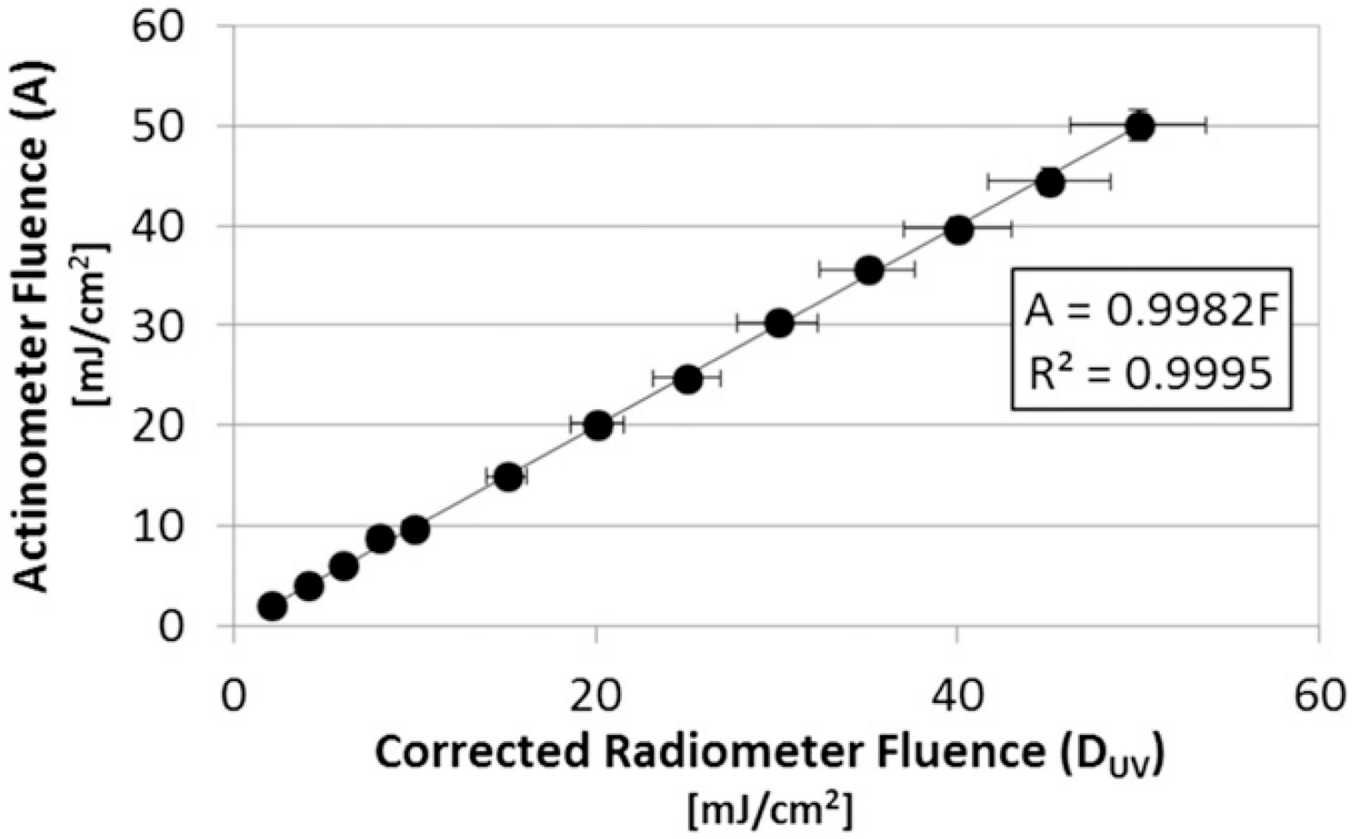

Fig. 4.

Actinometry fluence (UV dose) vs. UV dose determined using corrected radiometer readings (RF = 1.06); one test at 13 dose levels. The slope of 1 confirms the sample inside the quartz cuvettes are exposed to the same UV dose determined by the radiometer. Horizontal error bars represent the ±7.5% accuracy reported for the radiometer on the detector calibration certificates, while vertical error bars represent the ±3.1% uncertainty of the iodide-iodate actinometer reported by the U.S. National Institute of Standards and Technology (NIST) [15].

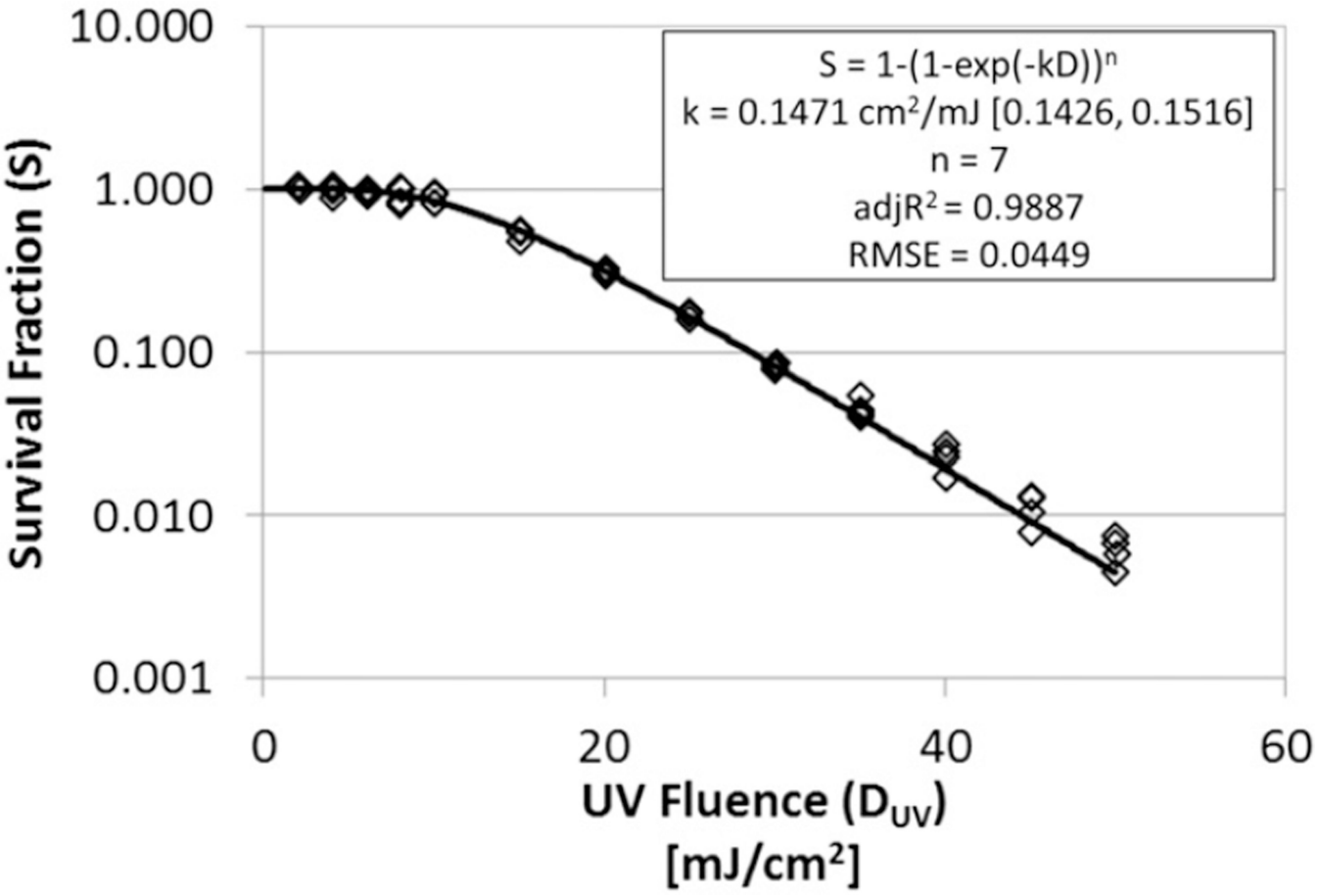

Fig. 5.

Best-fit exponential decay with a shoulder model (model 2) fit to the aqueous *Bacillus subtilis* data; four replicates at each of 13 dose levels.

Table 1

Common inactivation models for microbial populations exposed to ultraviolet energy.

Model number	Model details
1	**Simple exponential decay** [17,18]: $$S = e^{-kD_{UV}} \quad (7)$$ S represents the survival fraction (described above) of a microbiological population after exposure to a given UV dose (D_{UV}), and k is the species-dependent inactivation rate constant (cm^2/mJ).
2	**Exponential decay with a shoulder with n forced to be an integer** [19–21]: $$S = 1 - (1 - e^{-kD_{UV}})^n \quad (8)$$ Multi-hit model where n represents a discrete, species-dependent number of critical sites (targets) that must be hit by UV photons to completely inactivate the organism. Theoretically, n is an integer, but it is not always reported that way in scientific literature.
3	**Exponential decay with a shoulder with n allowed to be any real number** [19–21]: Same as Eq. (8) above
4	**Two-stage decay** [22,23]: $$S = (1 - f)e^{-k_1 D_{UV}} + fe^{-k_2 D_{UV}} \quad (9)$$ The resistant fraction of the microorganism population is designated (f) while the more susceptible fraction is (1 − f). Both population fractions have their own inactivation rate constants, designated k_1 and k_2 for (1 − f) and f, respectively.
5	**Two-stage decay with a shoulder with $n_1 = n_2$ and both forced to be integers** [17,21]: $$S = (1 - f)[1 - (1 - e^{-k_1 D_{UV}})^{n_1}] + f[1 - (1 - e^{-k_2 D_{UV}})^{n_2}]$$ A multi-hit model where n_1 represents a discrete number of targets that must be hit to inactivate the susceptible fraction of the population (1 − f) having a k-value of k_1 and n_2 is the number of hits to inactivate the resistant fraction (f) with a k-value of k_2.

Table 2

Inactivation rate constants (k-values) and multi-hit target numbers (n) for *Bacillus subtilis* spores in water published in the scientific literature. All k-values presented have been normalized to fit an exponential decay with a shoulder model.

k-Value (cm^2/mJ)	Target number (n)	Reference
0.147	7	This study (non-linear fit to multi-hit model shown in Fig. 5)
0.130	4.10	This study (linear approximation of multi-hit model)
0.304	1.85	Nedeljkovic-Davidovic [16]
0.385	2.33	Qualls and Johnson [24]
0.343	1.43	Mamane-Gravetz et al. [25]
0.237	0.81	Bohrerova et al. [26]
0.369	1.08	Bohrerova et al. [26]
0.145	1.34	Bohrerova et al. [26]
33.87	5	Deguchi et al. [27]